Original Article

MOLECULAR METABOLISM

Sema7A protects against high-fat diet-induced obesity and hepatic steatosis by regulating adipo/lipogenesis

Qiongyu Lu [1,5], Ziting Liu [1,5], Luyao Zhao [1,5], Linru Xu [1], Chu Liu [1], Ling Li [1], Yiren Cao [1], Fengchan Li [1], Lili Wu [1], Lei Wang [1], Ting Chen [1], Tao You [1], Lijie Ren [1], Guixue Wang [4,5], Chaojun Tang [1,2,3,4,**], Li Zhu [1,2,3,4,*]

ABSTRACT

Objective: Obesity and related diseases are becoming a growing risk for public health around the world due to the westernized lifestyle. Sema7A, an axonal guidance molecule, has been known to play a role in neurite growth, bone formation, and immune regulation. Whether Sema7A participates in obesity and metabolic diseases is unknown. As several SNPs in *SEMA7A* and its receptors were found to correlate with BMI and metabolic parameters in the human population, we investigated the potential role of Sema7A in obesity and hepatic steatosis.

Methods: GWAS and GEPIA database was used to analyze SNPs in *SEMA7A* and the correlation of Sema7A expression with lipid metabolism related genes. Sema7A$^{-/-}$ mice and recombinant Sema7A (rSema7A) were used to study the role of Sema7A in HFD-induced obesity and hepatic steatosis. Adipose tissue-derived mesenchymal stem cells (ADSCs) were used to examine the role of Sema7A in adipogenesis, lipogenesis and downstream signaling.

Results: Deletion of Sema7A aggravated HFD-induced obesity. Sema7A deletion enhanced adipogenesis in both subcutaneous and visceral ADSCs, while the addition of rSema7A inhibited adipogenesis of ADSCs and lipogenesis of differentiated mature adipocytes. Sema7A inhibits adipo/lipogenesis potentially through its receptor integrin β1 and downstream FAK signaling. Importantly, administration of rSema7A had protective effects against diet-induced obesity in mice. In addition, deletion of Sema7A led to increased hepatic steatosis and insulin resistance in mice.

Conclusions: Our findings reveal a novel inhibitory role of Sema7A in obesity and hepatic steatosis, providing a potential new therapeutic target for obesity and metabolic diseases.

Keywords Sema7A; Adipogenesis; Lipogenesis; ADSCs; Obesity; Hepatic steatosis

1. INTRODUCTION

Obesity and related diseases are becoming a growing risk for public health around the world due to the westernized lifestyle [1,2]. Excessive consumption of energy leads to the accumulation of lipids mainly in adipose tissue [3] and results in adipose inflammation, insulin resistance and type 2 diabetes [4]. Additionally, the enlarged adipose tissue releases excess free fatty acids that are taken up by hepatocytes and result in hepatic steatosis [2,4]. Increased blood lipid levels could also lead to atherosclerosis and cardiovascular and cerebrovascular diseases [1,5]. In the development of obesity, adipose tissue stores excessive lipids by inducing more lipid accumulation in mature adipocytes, which leads to expansion of adipocytes called hypertrophy, or by inducing adipogenesis, a process of generating new adipocytes. Multiple molecules have been reported to be involved in adipose hypertrophy and adipogenesis [6,7].

Semaphorins are a family originally identified as axonal guidance molecules that have been discovered from viruses, insects to mammals [8]. Semaphorins are involved in tumor growth, angiogenesis, immune regulation, and other biological and pathological processes. Several semaphorin 3 members are associated with hypothalamus-regulated obesity or related adipose tissue inflammation [9–12], while the role of other semaphorin members in

[1]Cyrus Tang Medical Institute, Cyrus Tang Hematology Center, Collaborative Innovation Center of Hematology of Jiangsu Province, Suzhou Key Lab of Thrombosis and Hemostasis, Jiangsu Key Laboratory of Preventive and Translational Medicine for Geriatric Diseases, Soochow University, Suzhou, China [2]National Clinical Research Center for Hematologic Diseases at the First Affiliated Hospital of Soochow University, Suzhou, Jiangsu, China [3]The Ninth Affiliated Hospital, Soochow University, Suzhou, Jiangsu, China [4]JinFeng Laboratory, Chongqing, China [5]Key Laboratory of Biorheological and Technology of Ministry of Education, State and Local Joint Engineering Laboratory for Vascular Implants, Bioengineering College of Chongqing University, Chongqing, China

[5] These authors contributed equally to this work.

*Corresponding author. Cyrus Tang Hematology Center, Soochow University, Building 709, Room 509, 199 Renai Road, Suzhou, Jiangsu, China 21512. E-mail: zhul@suda.edu.cn (L. Zhu).

**Corresponding author. Cyrus Tang Hematology Center, Soochow University, Building 709, Room 509, 199 Renai Road, Suzhou, Jiangsu, China 21512. E-mail: zjtang@suda.edu.cn (C. Tang).

Received January 7, 2023 • Revision received February 20, 2023 • Accepted February 20, 2023 • Available online 24 February 2023

https://doi.org/10.1016/j.molmet.2023.101698

Abbreviations

NAFLD	nonalcoholic fatty liver disease
ADSCs	adipose-derived mesenchymal stem cells
HFD	high-fat diet
Sema7A	semaphorin 7A
Itgb1	integrin β1
WAT	white adipose tissue
BAT	brown adipose tissue
SWAT	subcutaneous adipose tissue
pgWAT	perigonadal adipose tissue
rSema7A	recombinant Sema7A
SVF	stromal vascular fraction
BMI	body mass index
SNP	single nucleotide polymorphism

obesity has not been reported. Sema7A is a GPI-anchored semaphorin member involved in many immune-related diseases and regulates the function of macrophages, T cells and NK cells [13]. Sema7A also displays widespread expression outside the immune system and is involved in a variety of biological and pathological processes [14,15], including the regulation of bone function, neurite growth, angiogenesis [16], and atherosclerosis [17]. Sema7A has three known receptors, PlexinC1, integrin β1 and GPIb. Integrin β1 is reported to be expressed in mesenchymal stem cells and decreased during adipocyte differentiation [18]. Inhibition of integrin β1 leads to increased adipogenesis [19], and activation of the integrin β1-FAK pathway inhibits adipo/lipogenesis [20].

Bioinformatics analysis of the differentiation of mesenchymal stem cells into adipocytes implied that Sema7A may have a role in adipocyte differentiation [21]. Genome-wide association studies (GWAS) identified that SNPs of *SEMA7A* and its receptors were correlated with BMI and other metabolic parameters (https://www.gwascentral.org/). In this study, we proposed that Sema7A might participate in the pathogenesis of obesity and metabolic diseases. Using Sema7A$^{-/-}$ mice, we investigated the role of Sema7A in diet-induced obesity and found that Sema7A deficiency promoted obesity and hepatic steatosis in HFD mice. *In vitro* results showed that Sema7A inhibited adipogenesis of preadipocytes and lipogenesis of mature adipocytes. Administration of rSema7A protects against HFD-induced obesity in mice. Our findings reveal a role for Sema7A in lipid metabolism and provide a potential new therapeutic target for obesity.

2. MATERIALS AND METHODS

2.1. Animals

Sema7A$^{-/-}$ mice (C57BL/6J background) [22] were obtained from Jackson Laboratories (005128, Bar Harbor, USA) and backcrossed on C57BL/6 for >10 generations. All animals were kept in a pathogen-free facility with constant humidity, room temperature and 12 h light cycle. All animal studies were approved by the Institutional Animal Care and Use Committee of Soochow University.

For the role of Sema7A in HFD-induced obesity and hepatic steatosis, WT and Sema7A$^{-/-}$ mice were fed a high-fat (60%) diet (TP23300, Trophic Animal Feed High-Tech Co. Ltd. Nantong, China) or chow diet from the age of 8 weeks for 12–16 weeks and water ad libitum. For the therapeutic effect of rSema7A, Sema7A$^{-/-}$ female mice were injected with vehicle control or rSema7A intraperitoneally (35 μg/per mouse/per day) and fed HFD for 6 weeks.

2.2. Database search in GWAS CENTRAL and GEPIA

We searched SNPs in *SEMA7A* and its receptors *ITGB1* and *PLXNC1* and their correlation with BMI and other metabolic parameters using genome-wide association studies in GWAS CENTRAL (https://www.gwascentral.org/). SNPs that resulted in a phenotype difference of $P < 0.05$ were included in Table 1. We searched the correlation of SEMA7A and lipid metabolism-related genes in the GEPIA database (http://gepia.cancer-pku.cn/detail.php?clicktag=correlation).

2.3. Histological analysis

HE staining: Liver and adipose tissue were fixed with 4% paraformaldehyde solution in PBS and embedded in paraffin. Paraffin-embedded sections were stained with haematoxylin and eosin according to manufacturer's instructions and imaged with a Leica DM2000 microscope. Adipocyte areas were calculated with ImageJ.

Oil Red O staining of liver: Frozen sections of O.C.T. compound-embedded mouse livers were cut into 10 μm sections and fixed with 4% PFA. Oil Red O solutions in propylene glycol (O1516, Sigma) were used to stain neutral lipid droplets in frozen liver sections.

2.4. GTT and ITT

Glucose tolerance test (GTT): WT and Sema7A$^{-/-}$ mice on HFD were starved overnight with water ad libitum. Glucose (1.8 g/kg) was injected intraperitoneally, and blood glucose was monitored at the indicated time points with a OneTouch Ultra glucometer (Lifescan).

Insulin tolerance test (ITT): WT and Sema7A$^{-/-}$ mice on HFD were fed randomly. Insulin (Humulin, Lilly, 0.75 units/kg) was injected intraperitoneally, and blood glucose was monitored at the indicated time points with a OneTouch Ultra glucometer.

2.5. Coimmunoprecipitation and western blotting

Tissue and cell lysates prepared in RIPA buffer (1% Triton X-100, 1% deoxycholate, 0.1% SDS, 10 mM Tris and 150 mM NaCl) with protease and phosphatase inhibitor cocktail (Roche, USA) were separated with SDS-PAGE and probed with primary antibodies against P-ERK (20G11), ERK (9102), P-FAK (3283), FAK (3285), P-AKT Ser473 (D9E), Akt (C67E7), Acc1 (C83B10), and Fasn (C20G5) from CST and Srebp1 (2A4) from Santa Cruz. After incubation with primary antibodies at 4 °C overnight, membranes were incubated with fluorescent secondary antibodies (goat anti-rabbit IRDye 800CW, goat anti-mouse IRDye 800CW, Licor Odyssey, United States). Membranes were examined by an Odyssey infrared imaging system (LI-COR Biosciences, United States). For coimmunoprecipitation of Sema7A and Itgb1, ADSCs were incubated with 10 μg/mL Sema7A for 3 h and lysed with lysis buffer (P0013, Beyotime Biotechnology, China). The lysates were precleared with protein G and immunoprecipitated with Sema7A antibody (18070-1-AP, Proteintech) or IgG. The coimmunoprecipitated proteins and input sample were blotted with Itgb1 antibody (sc-374429, A4, Santa Cruz).

2.6. RNA isolation and qPCR

Total RNA was isolated from tissues and cells using TRIzol reagent (Invitrogen) and reverse transcribed into cDNA with Takara PrimeScript™ RT Master Mix (RR036A, Takara, Japan). Quantitative PCR was performed in 20 μL of the brilliant SYBR green PCR master mixture (4913914, Roche, Switzerland) in a real-time-PCR System

Table 1 — SNPs of *SEMA7A* and its receptors correlated with obesity and metabolic disorders.

Correlations with body mass index (BMI)							
SNP	Gene	p-value	Alleles	Position	Consequence	Amino acid	Dataset identifier
rs8036030	*SEMA7A*	0.04884	A>G,T	chr15:74424268 (GRCh38.p13)	Intron Variant		HGVRS570
rs8036030	*SEMA7A*	0.0374	A>G,T	chr15:74424268 (GRCh38.p13)	Intron Variant		HGVRS3271
rs11852686	*SEMA7A*	0.0174	T>A,C,G	chr15:74422864 (GRCh38.p13)	Intron Variant		HGVRS3271
rs11856835	*SEMA7A*	0.0201	G>A	chr15:74423833 (GRCh38.p13)	Intron Variant		HGVRS3271
rs1992145	*SEMA7A*	0.0313	G>A,C	chr15:74431303 (GRCh38.p13)	Intron Variant		HGVRS3271
rs2230394	*ITGB1*	0.01169	G>A,C	chr10:32928182 (GRCh38.p13)	Stop gained	NP_002202.2:p.Tyr153 = Y (Tyr) > * (Ter)	HGVRS569
rs2230394	*ITGB1*	0.01678	G>A,C	chr10:32928182 (GRCh38.p13)	Stop gained	NP_002202.2:p.Tyr153 = Y (Tyr) > * (Ter)	HGVRS570
rs2230395	*ITGB1*	0.01153	T>A,G	chr10:32922299 (GRCh38.p13)	Synonymous Variant	NP_002202.2:p.Ala362 = A (Ala) > A (Ala)	HGVRS569
rs9417094	*ITGB1*	0.01221	T>A,C	chr10:32938452 (GRCh38.p13)	Intron Variant		HGVRS569
rs2488326	*ITGB1*	0.01555	T>A,C	chr10:32918569 (GRCh38.p13)	Intron Variant		HGVRS570
rs1187070	*ITGB1*	0.0179	A>C	chr10:32952210 (GRCh38.p13)	Intron Variant		HGVRS570
rs10777584	*PLXNC1*	0.00596	C>A,G	chr12:94189373 (GRCh38.p13)	Intron Variant		HGVRS3271
rs10777585	*PLXNC1*	0.00577	A>C,G,T	chr12:94192937 (GRCh38.p13)	Intron Variant		HGVRS3271
rs3847804	*PLXNC1*	0.00294	C>G,T	chr12:94172522 (GRCh38.p13)	Intron Variant		HGVRS3271
rs4761590	*PLXNC1*	0.00518	C>G,T	chr12:94180035 (GRCh38.p13)	Intron Variant		HGVRS3271
rs12231028	*PLXNC1*	0.00821	C>A,T	chr12:94271277 (GRCh38.p13)	Intron Variant		HGVRS3271
Correlations with glycated hemoglobin levels							
SNP	Gene	p-value	Alleles	Position	Consequence	Amino acid	Dataset identifier
rs741761	*SEMA7A*	0.0008	T>A,C	chr15:74411588 (GRCh38.p13)	Missense Variant	NP_003603.1:p.Gln515 = Q (Gln) > H (His)	HGVRS3279
rs885740	*SEMA7A*	0.03997	G>A,C	chr15:74413341 (GRCh38.p13)	Intron Variant		HGVRS3279
rs17468	*ITGB1*	0.02909	G>A,T	chr10:32901357 (GRCh38.p13)	3 Prime UTR Variant		HGVRS3279
rs3824602	*ITGB1*	0.03964	C>A,T	chr10:32906949 (GRCh38.p13)	Intron Variant		HGVRS3279
rs2153871	*ITGB1*	0.02264	T>A,G	chr10:32928455 (GRCh38.p13)	Intron Variant		HGVRS3279
rs2230396	*ITGB1*	0.04959	G>C,T	chr10:32920338 (GRCh38.p13)	Synonymous Variant	NP_002202.2:p.Gly392 = G (Gly) > G (Gly)	HGVRS3279
rs2245840	*ITGB1*	0.02212	T>G	chr10:32935728 (GRCh38.p13)	Intron Variant		HGVRS3279
rs2488326	*ITGB1*	0.0203	T>A,C	chr10:32918569 (GRCh38.p13)	Intron Variant		HGVRS3279
rs2488328	*ITGB1*	0.04808	C>T	chr10:32924323 (GRCh38.p13)	Intron Variant		HGVRS3279
rs9417094	*ITGB1*	0.045	T>A,C	chr10:32938452	Intron Variant		HGVRS3279
Correlations with 2-h glucose challenge							
SNP	Gene	p-value	Alleles	Position	Consequence	Amino acid	Dataset identifier
rs1046146	*SEMA7A*	0.04552	G>A	chr15:74414602 (GRCh38.p13)	Synonymous Variant	NP_003603.1:p.Val413 = V (Val) > V (Val)	HGVRS3278
rs2075589	*SEMA7A*	0.01564	G>A,T	chr15:74417634 (GRCh38.p13)	Stop Gained	NP_003603.1:p.Tyr169 = Y (Tyr) > * (Ter)	HGVRS3278
rs2075591	*SEMA7A*	0.04773	C>A,G,T	chr15:74415652 (GRCh38.p13)	Intron Variant		HGVRS3278
rs12579612	plxnc1	0.01878	A>G	chr12:94272017 (GRCh38.p13)	Intron Variant		HGVRS3278
rs3894392	*PLXNC1*	0.02611	C>G,T	chr12:94164657 (GRCh38.p13)	Intron Variant		HGVRS3278
rs4237889	*PLXNC1*	0.03458	A>G,T	chr12:94155198 (GRCh38.p13)	Intron Variant		HGVRS3278
rs11834447	*PLXNC1*	0.04155	C>T	chr12:94268054 (GRCh38.p13)	Intron Variant		HGVRS3278
Correlations with insulin resistance							
SNP	Gene	p-value	Alleles	Position	Consequence	Amino acid	Dataset identifier
rs2734633	*SEMA7A*	0.03026	A>C,G	chr15:74415128 (GRCh38.p13)	Intron Variant		HGVRS3268
rs5015024	*SEMA7A*	0.034	G>A	chr15:74412247 (GRCh38.p13)	Intron Variant		HGVRS3268
rs10745681	*PLXNC1*	0.04572	G>T	chr12:94230927 (GRCh38.p13)	Intron Variant		HGVRS3268
rs10859690	*PLXNC1*	0.04884	G>A,C	chr12:94244533 (GRCh38.p13)	Intron Variant		HGVRS3268
rs12313726	*PLXNC1*	0.02852	T>C,G	chr12:94235911 (GRCh38.p13)	Intron Variant		HGVRS3268
rs12314236	*PLXNC1*	0.02683	T>C	chr12:94230737 (GRCh38.p13)	Intron Variant		HGVRS3268
rs7958289	*PLXNC1*	0.02794	G>A	chr12:94238250 (GRCh38.p13)	Intron Variant		HGVRS3268
rs7965633	*PLXNC1*	0.02774	T>C	chr12:94236739 (GRCh38.p13)	Intron Variant		HGVRS3268
rs7978182	*PLXNC1*	0.02486	A>C	chr12:94236195 (GRCh38.p13)	Intron Variant		HGVRS3268
rs7978522	*PLXNC1*	0.02398	C>G	chr12:94236432 (GRCh38.p13)	Intron Variant		HGVRS3268

(LightCycler 480, Roche, Switzerland). mRNA expression levels were calculated as relative fold changes by the 2-ΔΔCT method and normalized to 36B4 or actin mRNA levels in the same samples. Sequences for the qPCR primers are listed in Supplemental Table 1.

2.7. TG content in liver

WT or Sema7A$^{-/-}$ liver tissue was homogenized in lipid extraction solution (n-hepatane:isopropanol = 2:3.5, 4 mL for 400 mg tissue) with a homogenate and centrifuged. TG levels in the supernatant were tested using an assay kit from Nanjing Jiancheng Bioengineering Institute according to the manufacturer's instructions.

2.8. Analysis of blood lipids, leptin and insulin

Serum levels of TG (triglycerides), TC (total cholesterol), and LDL-C (low density lipoprotein) in overnight fasted mice were examined using assay kits from Nanjing Jiancheng Bioengineering Institute according to the manufacturer's instructions. Serum leptin and insulin levels were measured using ELISA kits according to the manufacturer's instructions (Raybio).

2.9. Adipogenesis assays

S-ADSCs (subcutaneous adipose-derived mesenchymal stem cells) and V-ADSCs (visceral adipose-derived mesenchymal stem cells) were isolated from inguinal adipose tissue or perigonadal adipose tissue as

previously described [23]. ADSCs were induced with differentiation media containing DMEM/F12 with 10% FBS, penicillin, streptomycin, 0.5 mM 3-isobutyl-1-methylxanthine (IBMX), 1 μM dexamethasone, 0.1 units/mL insulin and 1 μM rosiglitazone for 2 days and then cultured in induction medium containing DMEM/F12 with 10% FBS, penicillin, streptomycin and insulin for 6 days. Cells were then used for the indicated experiments.

The His-tagged recombinant mouse Sema7A (47—643) was purified using a Histrap™ HP (GE) column with an AKTA purifier. To block the FAK pathway, a FAK inhibitor (HY-12289A, MCE) was used at a final concentration of 5 μM.

Oil Red O staining of differentiated adipocytes: cells were fixed with 4% PFA and washed with PBS. The fixed cells were stained with Oil Red O for 30 min and washed with PBS and 50% ethanol. The red stained lipid droplets were photographed with a microscope and then extracted with isopropanol and quantified by absorbance at 518 nm.

2.10. Statistical analysis

Data were analyzed by Prism 8.0 (GraphPad) software with unpaired two-tailed Student's t tests or one-way ANOVA followed by post-HOC analysis. Data were presented as the mean ± SD (standard deviation) or as indicated in the figure legends. Differences were considered significant at $P < 0.05$.

3. RESULTS

3.1. SNPs in *SEMA7A* are correlated with metabolic parameters, and Sema7A is expressed in adipose tissue

Although Sema7A participates in many physiological and pathological processes, its role in obesity and metabolic diseases has not been reported. The only related information is that bioinformatics analysis of the differentiation of mesenchymal stem cells into adipocytes implied that Sema7A may have a role in adipocyte differentiation [21]. In this study, we searched SNPs located in *SEMA7A* and its receptors, *ITGB1* and *PLXNC1*, in GWAS CENTRAL (https://www.gwascentral.org/) and found dozens of SNPs correlated with metabolic parameters. As summarized in Table 1, four SNPs, rs8036030, rs11852686, rs11856835 and rs1992145, located on *SEMA7A*, which causes intron variants and does not affect amino acids, had a significant correlation with BMI ($P < 0.05$). Five SNP loci of *ITGB1* are correlated with BMI; among them, rs2230394 causes termination of translation (Tyr153 = Y (Tyr)>* (Ter)), and rs2230395 results in a synonymous variant of this protein. Five *PLXNC1* SNP loci (rs10777584, rs10777585, rs3847804, rs4761590, and rs12231028) were correlated with BMI ($P < 0.01$) (Table 1). SNPs of *SEMA7A* and its receptors are also correlated with glycated hemoglobin levels. Two SNP loci of *SEMA7A* are associated with glycated hemoglobin levels, with rs741761 causing a missense variant of Sema7A (missing Gln 515) ($P = 0.0008$) and rs885740 causing an intron variant. Eight *ITGB1* SNPs were correlated with glycated hemoglobin levels ($P < 0.05$). In addition, three SNPs of *SEMA7A* and four SNPs of *PLXNC1* were associated with a 2-h glucose challenge ($P < 0.05$), while two SNPs of *SEMA7A* and eight SNPs of *PLXNC1* were associated with insulin resistance ($P < 0.05$) (Table 1). These results implied a potential clinical relevance of Sema7A to obesity and metabolic diseases in the human population.

Sema7A is widely expressed in many tissues (brain, kidney, lung, etc.) and cells (endothelial cells, RBCs, macrophages, T cells, etc.). We next examined Sema7A expression in adipose tissue. We found that Sema7A is expressed in adipose tissue (Figure 1A) and mostly in endothelial cells or dendritic cells in adipose tissue by single-cell RNA sequencing (GSE161872) (Figure 1B). Sema7A expression seemed to decrease in most cell types (especially endothelial cells) of adipose tissue in mice on HFD (Figure 1B,C) or during adipogenesis in ADSCs (Figure 1D). By searching for a correlation of the expression of Sema7A with lipid metabolism-related genes in the GEPIA database, we found a negative correlation between the expression of Sema7A and lipid metabolism-related genes, including PPARG, PLIN1, FABP4, CEBPA and ADIPOQ in both subcutaneous adipose tissue (Figure 1E) and visceral adipose tissue (Figure 1F). Also, Sema7A expression was positively correlated with thermogenic genes, including DIO2 and PRDM16, in subcutaneous adipose tissue (Supplementary Fig. 1). Together, these data implied that Sema7A may be involved in the pathogenesis of obesity and metabolic diseases.

3.2. Deletion of Sema7A promoted high-fat diet-induced obesity

To ask whether Sema7A plays a role in obesity, we examined the effect of Sema7A deletion on HFD-induced obesity using Sema7A$^{-/-}$ mice. As expected, WT and Sema7A$^{-/-}$ mice on chow diet did not show a significant difference in the weights of SWAT, pgWAT or BAT (Supplementary Figs. 2A and B). However, body weights of both male and female Sema7A$^{-/-}$ mice on HFD were significantly higher than those of WT mice (Figure 2A). The fat mass, but not lean mass, in Sema7A$^{-/-}$ mice increased compared to that in WT mice (Figure 2B). For the white adipose tissue in female mice, the fat pad weights of inguinal subcutaneous adipose tissue (SWAT) and perigonadal visceral adipose tissue (pgWAT) in Sema7A$^{-/-}$ mice increased significantly compared to WT mice on HFD (Figure 2C,D), while in male mice, SWAT, but not pgWAT, increased significantly in Sema7A knockout mice on HFD (Figure 2D). HE staining showed enlarged adipocytes in SWAT and pgWAT in female Sema7A$^{-/-}$ mice (Figure 2E,F). For brown adipose tissue (BAT), weight increases were observed in both male and female mice (Figure 2G). BAT whitening was observed in Sema7A$^{-/-}$ mice fed HFD (Figure 2H). Metabolic measurements showed that Sema7A$^{-/-}$ mice had decreased O_2 consumption and CO_2 expiration (Supplementary Figs. 3A and B). There was no difference in overall food intake between WT and Sema7A$^{-/-}$ mice on chow diet or HFD (Supplementary Figs. 4A and B).

The blood lipid profile was examined in mice fed either chow diet or HFD after starving. In chow diet mice, only LDL-C showed an increase in Sema7A$^{-/-}$ mice compared with WT mice, while in HFD mice, TG, TC and LDL-C increased significantly in Sema7A$^{-/-}$ mice compared with WT mice (Figure 2I—K). Starved serum leptin levels were significantly increased in Sema7A$^{-/-}$ mice on HFD compared to WT mice (Figure 2L). Quantitative PCR assays showed that in HFD mice, the expression of lipogenesis genes, including Acss1 and Acc1, increased significantly in adipose tissue in Sema7A$^{-/-}$ mice (Figure 2M), while in mice fed chow diet, only Acss1 expression showed a slight increase in pgWAT in Sema7A$^{-/-}$ mice (Supplementary Figs. 5A and B). No significant difference in the expression of lipolysis genes in WT and Sema7A$^{-/-}$ mice on HFD was detected (Supplementary Figs. 6A and B). Additionally, Pparg in liver of Sema7A$^{-/-}$ mice on HFD was increased compared with that in WT mice (Figure 2N), which did not occur in mice on chow diet (Supplementary Fig. 5C).

The effect of Sema7A on spontaneous obesity in elderly (1 year on chow diet) mice was also observed. Results showed that Sema7A deletion led to increased body weights and the weights of SWAT, pgWAT, and BAT in both male and female mice (Supplementary Figs. 7A—E). Increased adipocyte size in white adipose tissue and whitening of BAT in elderly Sema7A$^{-/-}$ mice were observed (Supplementary Fig. 7G). Elderly Sema7A$^{-/-}$ mice showed

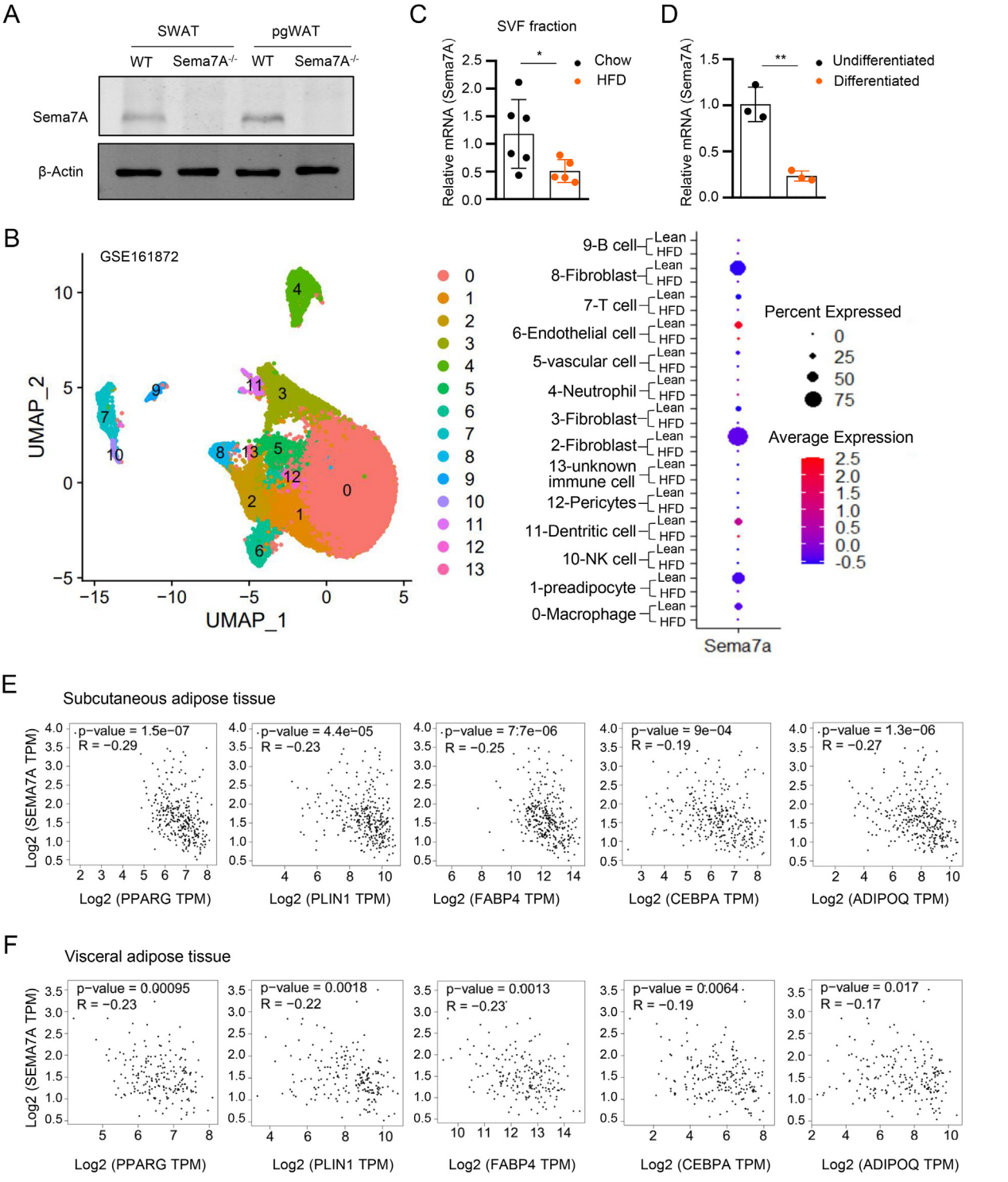

Figure 1: Expression of Sema7A in adipose tissue and correlation with adiposity. A. Expression of Sema7A in SWAT and pgWAT was detected by Western blotting. B. Sema7A expression in adipose tissue of lean (chow diet)- or HFD-fed mice searched in known scRNA-seq GEO datasets (GSE161872). C. Sema7A expression in the SVF fraction of adipose tissue in chow diet- or HFD-fed mice was examined by qPCR ($N \geq 5$ in each group). D. Expression of Sema7A in undifferentiated and differentiated ADSCs was measured with qPCR. E. Correlation of Sema7A expression to adiposity genes in normal subcutaneous adipose tissue was analyzed in the GEPIA database. F. Correlation of Sema7A and adiposity gene expression in normal visceral adipose tissue was analyzed in the GEPIA database. Data were presented as the mean ± SD. *$P < 0.05$, **$P < 0.01$.

enhanced liver weights with more lipid accumulation compared to WT mice (Supplementary Figs. 7F and H). Together, deletion of Sema7A promoted spontaneous obesity and hepatic steatosis in elderly mice.

3.3. Sema7A inhibited adipo/lipogenesis

To investigate how Sema7A affects obesity, we examined the role of Sema7A in adipogenesis. ADSCs were isolated from adipose tissue, and cell differentiation was induced for 8 days. Cells were then stained

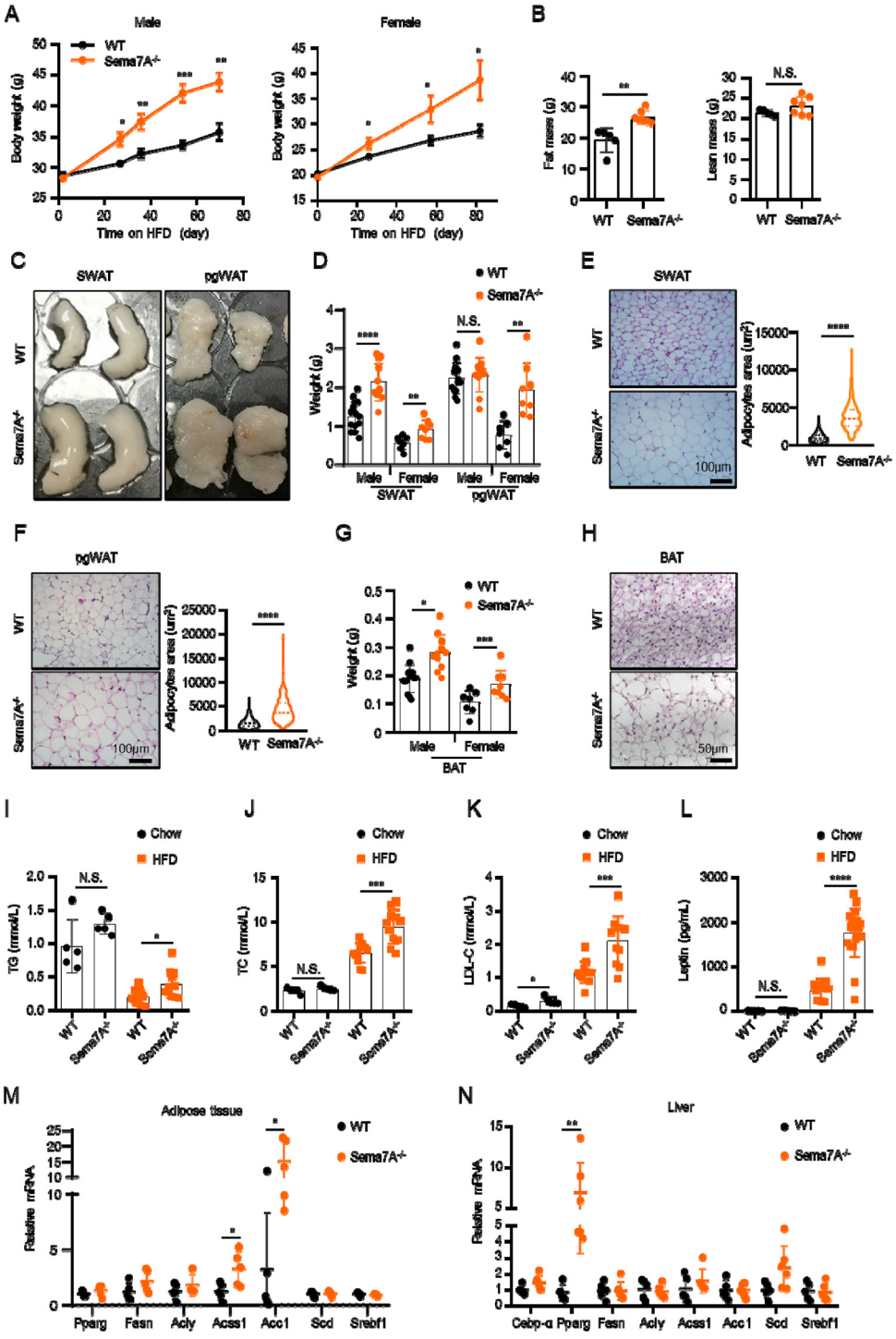

Figure 2: Deletion of Sema7A aggravated HFD-induced obesity. A. WT and Sema7A$^{-/-}$ mice were fed HFD from the age of 8 weeks and weighed at different time points ($N \geq 5$ in each group). B. Fat mass and lean mass of female mice on HFD for 5 months were analyzed using minispec TD-NMR (Bruker) ($N \geq 5$ in each group). C. WT and Sema7A$^{-/-}$ mice fed HFD for 12 weeks were sacrificed, and fat pads from different body parts were collected. Representative images of SWAT (subcutaneous adipose tissue) and pgWAT (perigonadal visceral adipose tissue) of female WT and Sema7A$^{-/-}$ mice were shown. D. Statistical analysis of the weights of fat pads of WT and Sema7A$^{-/-}$ mice on HFD for 12 weeks ($N \geq 7$ in each group). E&F. Representative HE staining images of SWAT (E) and pgWAT (F) from WT and Sema7A$^{-/-}$ female mice fed HFD were shown, of which the adipocyte area was statistically analyzed and shown with a violin plot. G. Statistical analysis of the weights of BAT from WT and Sema7A$^{-/-}$ mice on HFD ($N \geq 7$ in each group). H. Representative HE staining images of BAT from WT and Sema7A$^{-/-}$ male mice on HFD. I–K. Plasma lipid profiles, including TG (I), TC (J) and LDL-C (K), were measured ($N \geq 5$ in each group). L. Plasma leptin levels of starved and normal fed mice were measured with an ELISA kit ($N \geq 5$ in each group). M&N. The mRNA levels of lipogenesis genes in adipose tissue (M, $N \geq 4$ in each group) and liver (N, $N \geq 5$ in each group) from either WT or Sema7A$^{-/-}$ mice on HFD were examined with qPCR ($N \geq 5$ in each group). Data were shown as the mean ± SD. *$P < 0.05$, **$P < 0.01$, ***$P < 0.001$, ****$P < 0.0001$.

with Oil Red O that was extracted and quantified by the absorbance at 518 nm. Results showed that compared to WT controls, Sema7A deletion significantly enhanced lipid droplets in differentiated ADSCs isolated from subcutaneous adipose tissue (S-ADSCs) (Figure 3A) and visceral adipose tissue (V-ADSCs) (Figure 3B). In parallel, the effect of Sema7A on adipogenesis was examined using recombinant Sema7A (rSema7A, Supplementary Fig. 8A), which did not inhibit the proliferation of ADSCs (Supplementary Fig. 8B). Results showed that rSema7A inhibited adipogenesis in Sema7A$^{-/-}$ S-ADSCs or V-ADSCs after differentiation for 8 days (Figure 3C,D). The greatest inhibitory potency of rSema7A on adipogenesis of S-ADSCs occurred with the presence of rSema7A during day 0–2 of differentiation (Supplementary Fig. 8C).

We next examined the effect of Sema7A on the expression of adipogenic/lipogenic genes and showed that rSema7A inhibited the mRNA expression of Srebf1, Pparg, Acc1, Fasn, Acss1, Acly, Fabp4, Plin1 and Adipoq during adipogenesis of ADSCs (Figure 3E). We also examined the role of Sema7A in the lipogenesis of differentiated adipocytes and showed that rSema7A reduced both the mRNA and protein levels of lipogenesis genes in differentiated mature adipocytes (Figure 3F,G). These results suggest that Sema7A may protect against obesity by regulating adipo/lipogenesis. For brown adipocytes, we found an increase in adipogenesis and an elevation of lipogenic gene expression in Sema7A-deleted brown preadipocytes (Supplementary Figs. 9A and B). rSema7A promoted the expression of thermogenic genes and inhibited lipogenic gene expression in differentiated brown adipocytes (Supplementary Fig. 9C). In addition, a similar inhibitory effect of Sema7A on lipogenesis was observed in macrophages and endothelial cells (Supplementary Figs. 10A and B).

Sema7A has three known receptors, PlexinC1, integrin β1 and GPIb. Integrin β1 (Itgb1) was reported to be expressed in adipose-derived mesenchymal stem cells, and its inhibition leads to increased adipogenesis [19]. Consistently, we showed that integrin β1, but not PlexinC1 and GPIb, was highly expressed in ADSCs (Supplementary Fig. 11A). Blocking the binding of integrin β1 with Sema7A by RGD peptide enhanced lipid accumulation in ADSCs (Supplementary Fig. 11B). We therefore investigated whether Sema7A regulates adipo/lipogenesis through integrin β1 and its downstream signaling pathway. We first confirmed that integrin β1 expression decreased when ADSCs were differentiated (Figure 4A) and that Sema7A bound to integrin β1 by coimmunoprecipitation (Figure 4B). As Sema7A was reported to activate ERK through FAK signaling via integrin β1 receptor in immune cells [24] and in endothelial cells [17], integrin β1/FAK/ERK axis was examined. We found that rSema7A enhanced FAK phosphorylation in mature adipocytes purified from adipose tissue (Figure 4C). The inhibitory role of Sema7A on adipocyte lipogenesis was blocked by FAK inhibitor defactinib (Figure 4D–F). ERK phosphorylation during adipogenesis was decreased when Sema7A was deleted in ADSCs (Figure 4G), while the addition of rSema7A promoted ERK phosphorylation during adipogenesis (Figure 4H). These results suggested that Sema7A inhibits adipogenesis/lipogenesis through the integrin β1/FAK pathway (Figure 4I).

3.4. Deletion of Sema7A aggravated HFD-induced hepatic steatosis and insulin resistance

Nonalcoholic fatty liver disease (NAFLD) is a common complication of obesity [25]. We also examined the effect of Sema7A deletion on the progression of hepatic steatosis. Liver size and weight increased significantly in Sema7A$^{-/-}$ mice compared to WT mice on HFD for 16 weeks (Figure 5A,B). Relatively more lipid accumulation with larger lipid droplets was observed in Sema7A knockout mice on HFD than in WT mice (Figure 5C). Moreover, Sema7A deletion enhanced the HFD-induced increase in liver triglycerides (Figure 5D) but did not change plasma levels of AST and ALT, signs of liver damage (Supplementary Figs. 12A and B).

Obesity often results in systemic glucose intolerance and insulin resistance [26], and adipose and systemic inflammation are important causes of insulin resistance. To determine whether deletion of Sema7A affects HFD-induced adipose and liver inflammation, we determined the expression of markers for macrophage polarization in adipose tissue and liver of WT and Sema7A$^{-/-}$ mice with qPCR. In both adipose tissue and liver, increases in M1 polarization markers such as TNFα and IL6 and decreases in M2 markers such as IL10 and CD301 were observed in Sema7A$^{-/-}$ mice compared to WT mice (Supplementary Figs. 13A–C).

To investigate the role of Sema7A in obesity-related glucose tolerance and insulin resistance, mice fed HFD were challenged with high concentrations of D-glucose and insulin, and blood glucose levels were monitored. Results showed that Sema7A deletion led to more severe glucose intolerance and insulin resistance (Figure 5E,F), while serum insulin levels showed no significant difference (Figure 5G). To test whether deletion of Sema7A affects AKT signaling downstream of insulin, mice on HFD were fasted overnight and injected with 0.75 unit/kg insulin. Adipose tissue was isolated 15 min after insulin injection. Western blotting showed decreased AKT phosphorylation in Sema7A$^{-/-}$ mice compared to WT mice (Figure 5H). The liver was isolated 5 min after 1.0 units/kg insulin injection of fasted mice, and Western blotting showed decreased AKT phosphorylation in the liver of Sema7A$^{-/-}$ mice compared to WT mice (Figure 5I). Together, these data suggest that deletion of Sema7A leads to increased insulin resistance.

3.5. Recombinant Sema7A had protective effects against diet-induced obesity in mice

As deletion of Sema7A enhanced HFD- and age-induced obesity in mice, and Sema7A from red blood cells, immune cells and endothelial cells could be cleaved and released as soluble Sema7A in plasma, we propose that administration of rSema7A may have a protective effect against HFD-induced obesity. To test our hypothesis, three groups of female mice were arranged: WT mice, Sema7A$^{-/-}$ mice injected with PBS (vehicle control) or rSema7A (35 μg/per mouse/per day) intraperitoneally along with HFD feeding for 6 weeks and weighed weekly (Figure 6A). As illustrated in Figure 6B,C, the body weights of Sema7A$^{-/-}$ mice injected with PBS increased faster than those of WT mice, while the Sema7A$^{-/-}$ mice treated with rSema7A had a smaller body weight increase than those treated with the vehicle control. The percentage of body weight increase in Sema7A$^{-/-}$ mice started to be significantly inhibited at week 3 after rSema7A treatment compared with the vehicle control group (Figure 6C, $P < 0.05$). At 6 weeks after rSema7A treatment, the body weight gain by HFD in the rSema7A-treated group (27.93% ± 4.0) showed a relatively larger decrease compared to the PBS-treated group (45.01% ± 10.40) in the Sema7A$^{-/-}$ mice ($P < 0.05$, $N \geq 5$) (Figure 6C). For the white adipose tissue in mice, the fat pad weights of pgWAT and perirenal WAT decreased in mice treated with rSema7A compared to mice treated with vehicle control (Figure 6D–F). HE staining showed a reduced size of adipocytes in perirenal visceral adipose tissue of mice treated with rSema7A compared with mice treated with vehicle control (Figure 6G). These results indicated that rSema7A had protective effects against diet-induced obesity in mice.

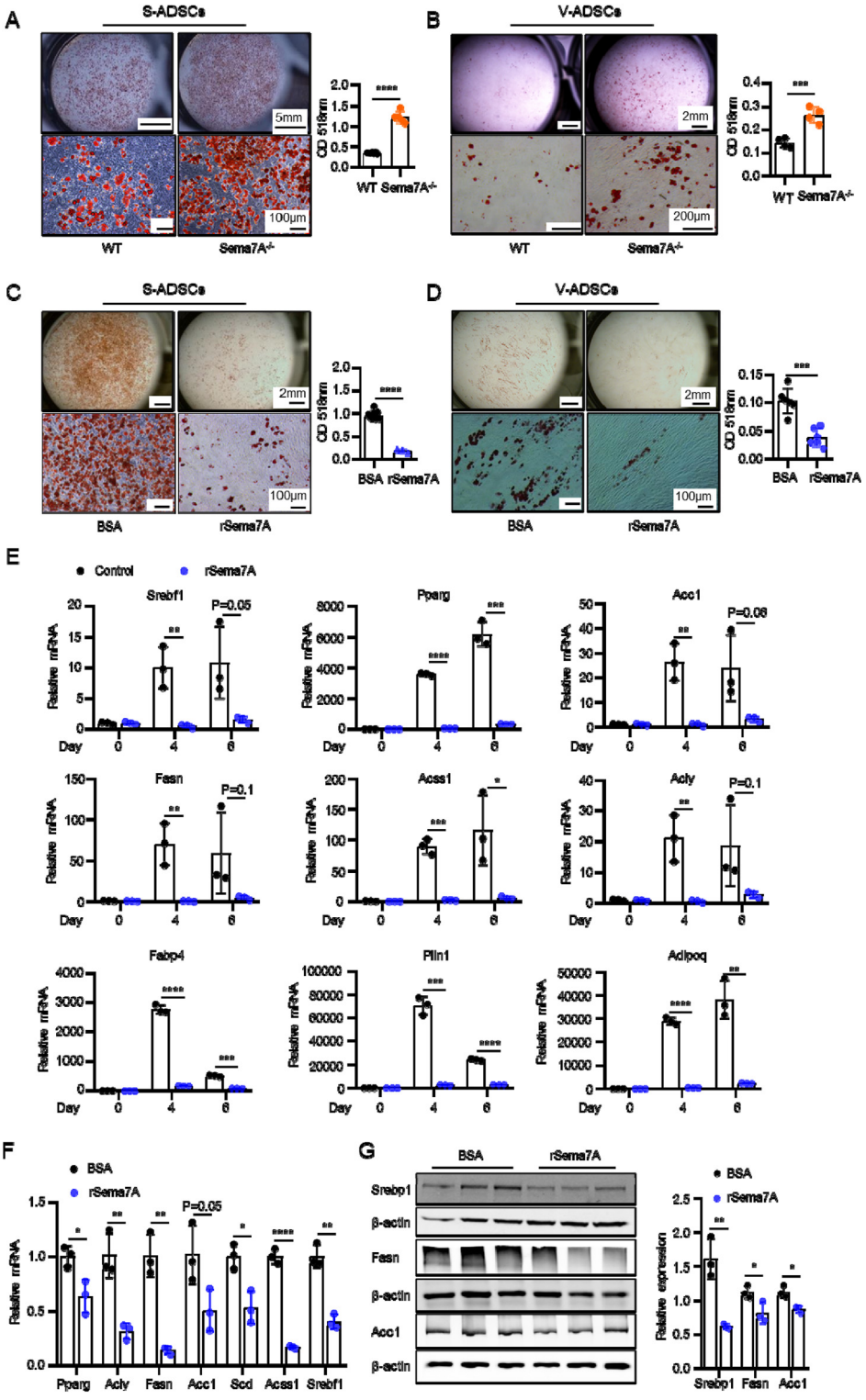

Figure 3: Sema7A inhibited adipogenesis/lipogenesis. A. S-ADSCs were isolated from subcutaneous adipose tissue of both WT and Sema7A$^{-/-}$ mice at the age of 3–6 weeks and induced with adipocyte differentiation medium. Cells were stained with Oil Red O after 8 days of differentiation. Oil Red O was extracted with isopropanol and quantified by the absorbance at 518 nm. B. V-ADSCs were isolated from visceral adipose tissue of both WT and Sema7A$^{-/-}$ mice at the age of 3–6 weeks, induced with adipocyte differentiation medium, and stained with Oil Red O at the end of differentiation. C. S-ADSCs were treated with or without rSema7A and differentiated into adipocytes. D. Sema7A$^{-/-}$ V-ADSCs were treated with or without rSema7A and differentiated into adipocytes. E. ADSCs were treated with or without rSema7A and induced for adipocyte differentiation. mRNA expression of adipo/lipogenic genes at day 0, 4, or 6 was detected with qPCR. F&G. Differentiated mature adipocytes were incubated with or without rSema7A for 24 h, and the mRNA (F) and protein (G) levels of lipogenesis genes were tested with qPCR and Western blotting. Data were presented as mean ± SD. *P < 0.05, **P < 0.01, ***P < 0.001, ****P < 0.0001.

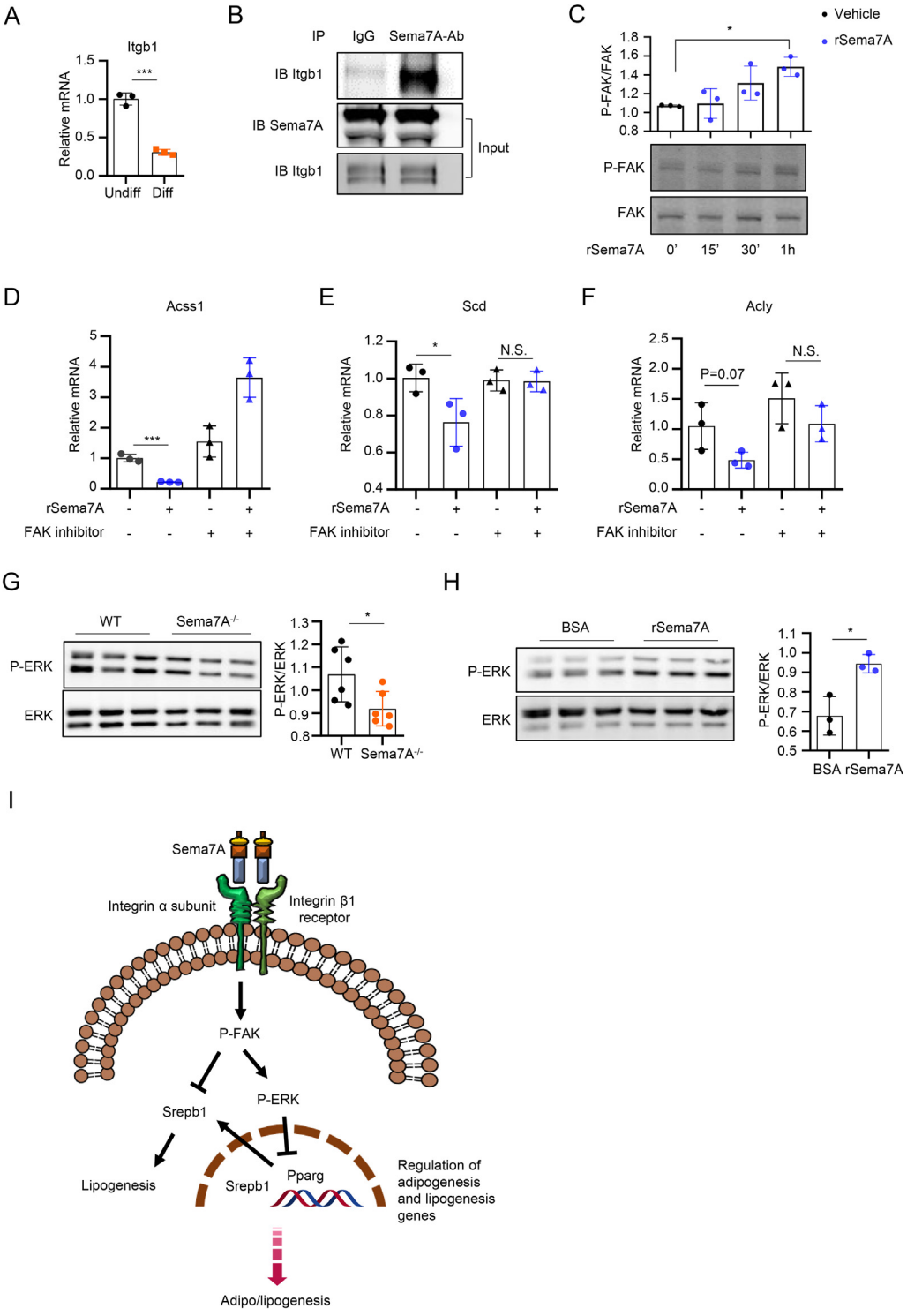

Figure 4: Sema7A inhibited adipo/lipogenesis potentially via the integrin β1/FAK signaling pathway. A. Expression of Itgb1 in undifferentiated and differentiated ADSCs was measured with qPCR. B. ADSCs were incubated with rSema7A for 3 h. The lysates were immunoprecipitated with Sema7A antibody and immunoblotted with Itgb1 antibody. C. Adipose tissue was digested using collagenase and centrifuged. Mature adipocytes were collected and starved for 5 h followed by incubation with rSema7A for the indicated times. Phosphorylation of the FAK signaling pathway was tested with Western blotting. D-F. Differentiated mature adipocytes incubated with or without FAK inhibitor were treated with rSema7A for 24 h, and lipogenesis genes were measured with qPCR. G. WT and Sema7A$^{-/-}$ ADSCs were induced with adipocyte differentiation medium, and protein samples during day 2 of differentiation were tested for ERK phosphorylation by Western blotting. H. ADSCs were differentiated into adipocytes in the presence or absence of rSema7A, and phosphorylation of ERK on day 2 of differentiation was tested with Western blotting. I. Proposed mechanism of the role of Sema7A in adipogenesis/lipogenesis. Sema7A binds to integrin β1 and activates downstream FAK/ERK signaling, inhibiting downstream Srebp1 and Pparg and adipo/lipogenesis. Data were presented as the mean ± SD. *P < 0.05, ***P < 0.001.

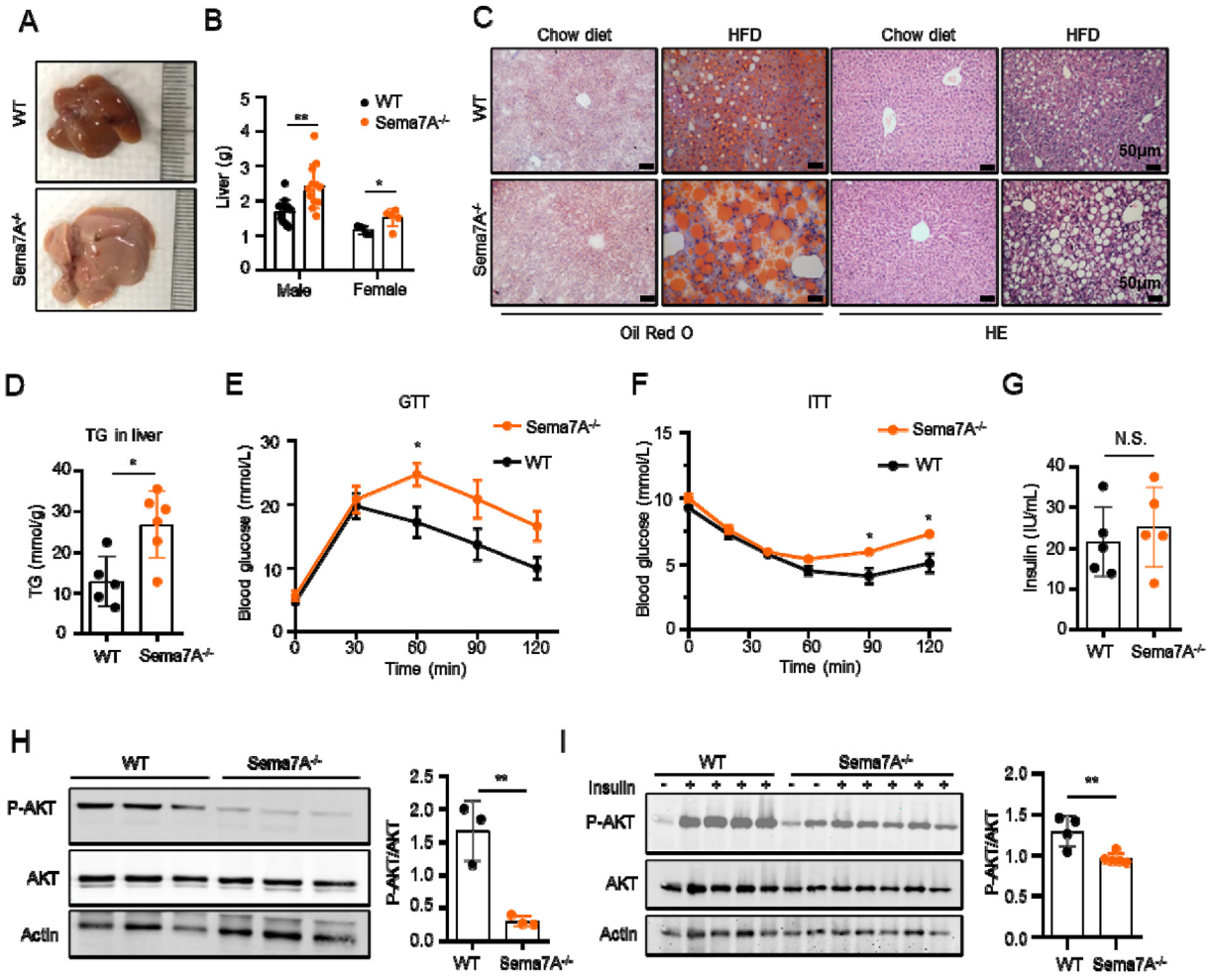

Figure 5: Deletion of Sema7A aggravated high fat diet induced hepatic steatosis and insulin resistance. A. Representative image of female WT and Sema7A−/− mice on HFD. B. Livers from both male and female WT and Sema7A$^{-/-}$ mice on HFD were weighed (N $\geq$ 5 in each group). C. Frozen liver sections of WT and Sema7A$^{-/-}$ mice fed chow diet or HFD were stained with Oil Red O, and paraffin-embedded sections were stained with HE. D. TG (Triacylglycerol) in liver tissues of WT and Sema7A$^{-/-}$ mice on HFD (N $\geq$ 5 in each group). E. WT and Sema7A$^{-/-}$ mice fed HFD were starved overnight, and 1.8 g/kg glucose was injected intraperitoneally for the glucose tolerance test (GTT). Blood glucose levels were monitored at the indicated time points (n = 5 for each group). F. Mice were fed ad libitum, and 0.75 units/kg insulin was injected intraperitoneally for the insulin tolerance test (ITT). Blood glucose levels were monitored at the indicated time points (n = 6 for each group). G. Fasted insulin levels in WT and Sema7A$^{-/-}$ mice on HFD were measured using an ELISA kit (N = 5 in each group). H. WT and Sema7A$^{-/-}$ mice on HFD were starved overnight and injected with insulin. Fifteen minutes after injection, adipose tissue was collected, and activation of AKT downstream insulin signaling was detected by Western blotting ((N = 3 in each group). I. WT and Sema7A$^{-/-}$ mice on HFD were starved overnight and injected with 1 unit/kg insulin. Five minutes after injection, livers were dissected, and activation of AKT downstream of insulin signaling was detected by Western blotting. Phosphorylation of AKT in insulin stimulated WT and Sema7A−/− liver were calculated with ImageJ (N $\geq$ 4 in each group). Data in E and F were presented as the mean $\pm$ SEM. Other data were presented as the mean $\pm$ SD. *P $<$ 0.05, **P $<$ 0.01.

4. DISCUSSION

Due to the westernized lifestyle, obesity is becoming a growing risk for public health around the world. Based on the database search that SNPs in Sema7A are correlated with metabolic parameters, we investigated the role of Sema7A in obesity. We showed that Sema7A deficiency enhanced diet-induced obesity with increased blood lipid levels and lipogenic gene expression. Supportively, Sema7A-deficient ADSCs showed increased adipogenesis, while rSema7A inhibited adipogenesis of preadipocytes and lipogenesis of mature adipocytes. Deletion of Sema7A also enhanced hepatic steatosis and increased insulin resistance in mice. Finally, administration of rSema7A protected against HFD-induced obesity in mice.

Semaphorins belong to the axonal guidance molecules and are involved in the regulation of axonal guidance. Numerous studies have reported the role of semaphorins outside the nervous system, such as immune regulation, angiogenesis, and bone formation. Obesity is a metabolic disorder resulting from the imbalance of the complex regulatory network containing multiple organs, cells and proteins. Current knowledge of the involvement of semaphorins (mostly semaphorin 3) in obesity and metabolic disorders includes the following three progresses. First, semaphorin 3 signaling regulates obesity by promoting the development of hypothalamic circuits. Human variants of semaphorin 3 and their receptors are associated with obesity [9]. Second, Sema3E is reported to be associated with macrophage recruitment and adipose tissue inflammation in obesity [10]. Third, Sema3A has been reported to play an inhibitory role in adipogenesis [12], while Sema3G enhances adipogenesis. Moreover, Sema3G knockdown ameliorates obesity, fatty liver and insulin resistance in mice on HFD [27]. In this study, we examined the potential role of Sema7A, the only GPI-

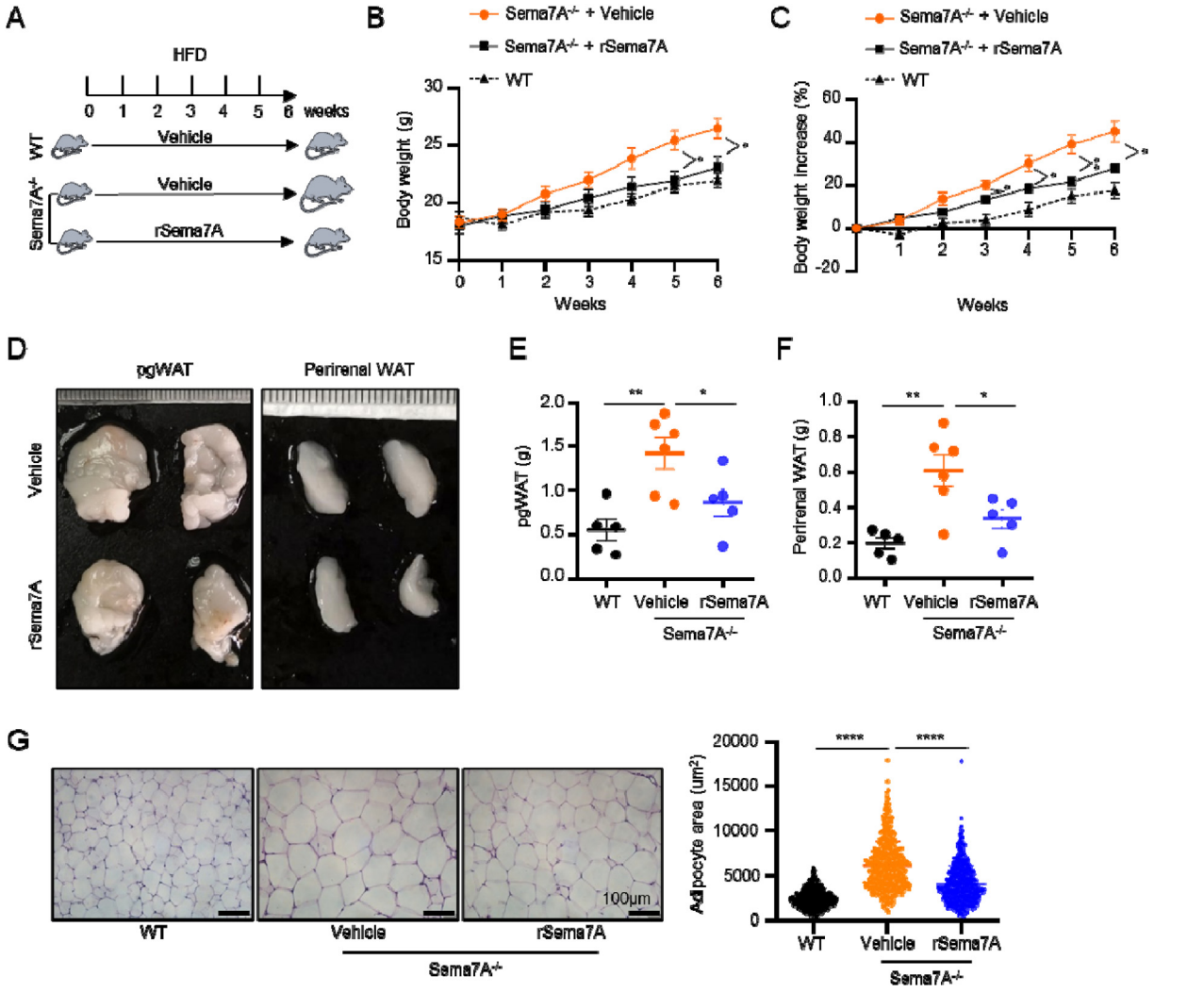

Figure 6: Recombinant Sema7A protected against diet-induced obesity. A. An experimental design to evaluate the effect of rSema7A on diet-induced obesity. B&C. Sema7A$^{-/-}$ female mice were treated with vehicle control or rSema7A intraperitoneally and weighed weekly. Increases in the body weights of WT mice and Sema7A$^{-/-}$ mice treated with vehicle control or rSema7A ($n \geq 5$) were analyzed. D. Representative images of pgWAT and perirenal WAT of mice treated with control or rSema7A. E-F. Weights of pgWAT (E) and perirenal WAT (F) of WT and Sema7A$^{-/-}$ mice treated with rSema7A or control. G. Representative images of HE staining of perirenal visceral adipose tissue of WT and Sema7A$^{-/-}$ mice treated with vehicle control or rSema7A. The area of approximately 500 adipocytes in each group was quantified using ImageJ. Data in B and C were presented as the mean ± SEM. Other data were presented as the mean ± SD. *P < 0.05, **P < 0.01, ****P < 0.0001.

anchored semaphorin member, in adipogenesis and obesity. We showed that Sema7A protects against HFD-induced obesity and hepatic steatosis, probably by regulating adipogenesis and lipogenesis. Sema7A was found on the surface of red blood cells and considered John Milton Hagen blood antigen [28]. Sema7A is also widely expressed in many tissue and cell types, including brain, lung, endothelial cells, macrophages and T cells. In this study, we found that Sema7A is expressed in adipose tissue and mostly on endothelial cells within adipose tissue by scRNA-seq (GSE161872). Sema7A expression decreased during adipogenesis, and its expression on the surface of red blood cells also decreased in elderly people [14]. Because of the wide expression of Sema7A, the exact origin of the role of Sema7A in obesity is unclear. Cell- and tissue-specific depletion of Sema7A may help to further study the origin and mechanism. Sema7A has been identified to be cleaved by MMPs and released from cells rapidly to become soluble Sema7A [29]. The protective effect of recombinant Sema7A against HFD-induced obesity in this study implies that Sema7A could come from shedding from red blood cells, macrophages, and endothelial cells and be released into the circulation as soluble Sema7A. Whether brain Sema7A or local endothelial Sema7A within adipose tissue plays a role in obesity is an open question.

Sema7A is a GPI-anchored protein that binds to receptors, including PlexinC1, Itgb1 and GPIb. Given that GPIb and PlexinC1 were barely detectable in ADSCs, we focused on Itgb1-mediated signaling in regulating lipid metabolism, which also mediates the role of Sema7A in metabolism, oxidative phosphorylation and glycolysis of macrophages [30]. Integrin β1 is reported to be expressed in mesenchymal stem cells and decreased after adipocyte differentiation [18]. Inhibition of integrin β1 leads to increased adipogenesis [19], and activation of the integrin β1-FAK pathway inhibits adipo/lipogenesis [20]. In our study, we also showed that Sema7A bound to integrin β1 and that inhibition of downstream FAK signaling blocked the inhibitory effect of Sema7A on lipogenesis. FAK activation is reported to activate ERK signaling and

inhibit srebp1 and pparg expression, which leads to the expression of adipogenesis and lipogenesis genes. We found a stimulatory role of Sema7A in ERK phosphorylation (which negatively regulates adipogenesis) during adipogenesis. However, an in-depth understanding of the interaction of Sema7A with integrin and the downstream signaling pathway in regulating adipogenesis and lipid metabolism in adipocytes needs further investigation.

In our study, we also found that Sema7A deletion led to whitening of brown adipose tissue in HFD and elderly mice, implying that Sema7A may regulate brown adipose metabolism. In vitro results showed that Sema7A inhibited lipogenesis and stimulated thermogenesis in brown adipocytes. These results suggest that the regulatory role of beige and brown adipose tissue may also be a contributing factor for their role in obesity. The regulation of Sema7A in lipogenesis was also observed in macrophages and endothelial cells, suggesting that the role of Sema7A in metabolism might be independent of cell type. A recent report showed that Sema7A regulates oxidative phosphorylation and glycolysis in macrophages [30], indicating its potential role in regulating metabolism in other cells. Whether Sema7A regulates thermogenesis of beige adipocytes and skeletal muscle and the underlying mechanism are warranted for a further investigation.

NAFLD is an important complication of obesity [31], which might lead to nonalcoholic hepatitis, hepatic fibrosis and even liver cancer. In this study, we found more severe diet-induced hepatic steatosis when Sema7A was deleted, which might also contribute to the weight increase in Sema7A$^{-/-}$ mice. Lipids deposited in the liver could be derived from diet, circulating fatty acids released from adipose tissue, and de novo lipogenesis. Circulating fatty acids account for approximately 60% of the hepatic triglyceride content in NAFLD [32], and obesity results in elevation of circulating fatty acids [32,33]. Hence, increased hepatic steatosis in Sema7A-deleted mice may partly result from obesity. De novo lipogenesis also plays a substantial role in the pathogenesis of NAFLD, accounting for 26% of hepatic triglycerides [32]. Quantitative PCR results showed increased expression of lipogenic genes in the livers of Sema7A$^{-/-}$ mice, implying that Sema7A might also participate in de novo lipogenesis in the liver, which deserves further investigation.

We noticed that pgWAT did not change in Sema7A$^{-/-}$ male mice on HFD, although the weights of sWAT, pgWAT and BAT all increased in Sema7A$^{-/-}$ female mice on HFD. This gender difference in response to Sema7A deficiency could be due to multiple factors. First, many genes regulate metabolic phenotypes differently in different genders. For example: Lypla11 knock out only protects against diet induced obesity in female mice, but not in male mice (Knockout of murine Lyplal1 confers sex-specific protection against diet-induced obesity, bioRxiv, posted 8.05.2021). Tmem18 knockout male mice show increased obesity, while female mice show no difference [34]. Hepatic steatosis was observed in igf1-deficient male zebrafish but not in female fish [35]. Second, hormone differences are believed to be an important influencing factor for metabolic differences in male and female mice [36,37]. Although most researchers have used male mice in experiments for consistency, increasing evidence indicates that both genders have been used to study the role of genes or medications in metabolic diseases.

In summary, we have identified a new role of Sema7A in obesity and hepatic steatosis. SNPs in Sema7A are correlated with metabolic parameters in the human population. Moreover, administration of rSema7A protected against HFD-induced obesity in mice. Although a further understanding of how Sema7A plays its role in obesity is required for its translational study, our findings open a new research direction for investigating obesity and related metabolic diseases, providing a potential new prophylaxis and therapeutic target.

AUTHOR CONTRIBUTIONS

Qiongyu Lu designed the project, performed experiments and wrote the original draft. Ziting Liu and Luyao Zhao performed the experiments and analysis. Linru Xu, Chu Liu, and Ling Li performed the experiments. Yiren Cao, Fengchan Li, Lei Wang, Lili Wu and Ting Chen helped with animal breeding and experiments. Tao You, Chaojun Tang and Lijie Ren helped with data analysis. Guixue Wang revised and edited the manuscript. Li Zhu designed the project, revised and edited the manuscript, and provided funding for this project. Prof. Li Zhu is the guarantor of this work and, as such, had full access to all the data in the study and takes responsibility for the integrity of the data and the accuracy of the data analysis.

FUNDING

This work was supported by the Natural Science Foundation of China (82170466, 81500653, and 82070450), Suzhou Science and Technology Development Project (SKY2022109, SKJY2021051), the Translational Research Grant of NCRCH (2020ZKPA01), the Postgraduate Research & Practice Innovation Program of Jiangsu Province (KYCX22_3216) and the Priority Academic Program Development of Jiangsu Higher Education Institutions of China.

CONFLICT OF INTEREST

The authors declare that they have no conflicts of interest.

DATA AVAILABILITY

Data will be made available on request.

APPENDIX A. SUPPLEMENTARY DATA

Supplementary data to this article can be found online at https://doi.org/10.1016/j.molmet.2023.101698.

REFERENCES

[1] De Lorenzo A, Gratteri S, Gualtieri P, Cammarano A, Bertucci P, Di Renzo L. Why primary obesity is a disease? J Transl Med 2019;17:169.
[2] Yazici D, Sezer H. Insulin resistance, obesity and lipotoxicity. Adv Exp Med Biol 2017;960:277–304.
[3] Wilborn C, Beckham J, Campbell B, Harvey T, Galbreath M, La Bounty P, et al. Obesity: prevalence, theories, medical consequences, management, and research directions. J Int Soc Sports Nutr 2005;2:4–31.
[4] Kawai T, Autieri MV, Scalia R. Adipose tissue inflammation and metabolic dysfunction in obesity. Am J Physiol Cell Physiol 2021;320:C375–91.
[5] Schetz M, De Jong A, Deane AM, Druml W, Hemelaar P, Pelosi P, et al. Obesity in the critically ill: a narrative review. Intensive Care Med 2019;45:757–69.
[6] Mota de Sa P, Richard AJ, Hang H, Stephens JM. Transcriptional regulation of adipogenesis. Compr Physiol 2017;7:635–74.
[7] Ghaben AL, Scherer PE. Adipogenesis and metabolic health. Nat Rev Mol Cell Biol 2019;20:242–58.
[8] Yazdani U, Terman JR. The semaphorins. Genome Biol 2006;7:211.

[9] van der Klaauw AA, Croizier S, Mendes de Oliveira E, Stadler LKJ, Park S, Kong Y, et al. Human semaphorin 3 variants link melanocortin circuit development and energy balance. Cell 2019;176:729–742 e718.
[10] Shimizu I, Yoshida Y, Moriya J, Nojima A, Uemura A, Kobayashi Y, et al. Semaphorin3E-induced inflammation contributes to insulin resistance in dietary obesity. Cell Metabol 2013;18:491–504.
[11] Mejhert N, Wilfling F, Esteve D, Galitzky J, Pellegrinelli V, Kolditz CI, et al. Semaphorin 3C is a novel adipokine linked to extracellular matrix composition. Diabetologia 2013;56:1792–801.
[12] Liu X, Tan N, Zhou Y, Zhou X, Chen H, Wei H, et al. Semaphorin 3A shifts adipose mesenchymal stem cells towards osteogenic phenotype and promotes bone regeneration in vivo. Stem Cell Int 2016;2016:2545214.
[13] Garcia-Areas R, Libreros S, Iragavarapu-Charyulu V. Semaphorin7A: branching beyond axonal guidance and into immunity. Immunol Res 2013;57:81–5.
[14] Kohler D, Granja T, Volz J, Koeppen M, Langer HF, Hansmann G, et al. Red blood cell-derived semaphorin 7A promotes thrombo-inflammation in myocardial ischemia-reperfusion injury through platelet GPIb. Nat Commun 2020;11:1315.
[15] Inoue N, Nishizumi H, Naritsuka H, Kiyonari H, Sakano H. Sema7A/PlxnCl signaling triggers activity-dependent olfactory synapse formation. Nat Commun 2018;9:1842.
[16] Hu S, Liu Y, You T, Zhu L. Semaphorin 7A promotes VEGFA/VEGFR2-Mediated angiogenesis and intraplaque neovascularization in ApoE(-/-) mice. Front Physiol 2018;9:1718.
[17] Hu S, Liu Y, You T, Heath J, Xu L, Zheng X, et al. Vascular semaphorin 7A upregulation by disturbed flow promotes atherosclerosis through endothelial beta1 integrin. Arterioscler Thromb Vasc Biol 2018;38:335–43.
[18] Frith JE, Mills RJ, Hudson JE, Cooper-White JJ. Tailored integrin-extracellular matrix interactions to direct human mesenchymal stem cell differentiation. Stem Cell Dev 2012;21:2442–56.
[19] Chen Q, Shou P, Zhang L, Xu C, Zheng C, Han Y, et al. An osteopontin-integrin interaction plays a critical role in directing adipogenesis and osteogenesis by mesenchymal stem cells. Stem Cell 2014;32:327–37.
[20] Yau SW, Russo VC, Clarke IJ, Dunshea FR, Werther GA, Sabin MA. IGFBP-2 inhibits adipogenesis and lipogenesis in human visceral, but not subcutaneous, adipocytes. Int J Obes 2015;39:770–81.
[21] Xu X, Jiang H, Li X, Wu P, Liu J, Wang T, et al. Bioinformatics analysis on the differentiation of bone mesenchymal stem cells into osteoblasts and adipocytes. Mol Med Rep 2017;15:1571–6.
[22] Pasterkamp RJ, Peschon JJ, Spriggs MK, Kolodkin AL. Semaphorin 7A promotes axon outgrowth through integrins and MAPKs. Nature 2003;424:398–405.
[23] Smith NC, Fairbridge NA, Pallegar NK, Christian SL. Dynamic upregulation of CD24 in pre-adipocytes promotes adipogenesis. Adipocyte 2015;4:89–100.
[24] Jongbloets BC, Ramakers GM, Pasterkamp RJ. Semaphorin7A and its receptors: pleiotropic regulators of immune cell function, bone homeostasis, and neural development. Semin Cell Dev Biol 2013;24:129–38.
[25] Polyzos SA, Kountouras J, Mantzoros CS. Obesity and nonalcoholic fatty liver disease: from pathophysiology to therapeutics. Metabolism 2019;92:82–97.
[26] Choi CHJ, Cohen P. How does obesity lead to insulin resistance? Elife 2017;6.
[27] Liu M, Xie S, Liu W, Li J, Li C, Huang W, et al. Mechanism of SEMA3G knockdown-mediated attenuation of high-fat diet-induced obesity. J Endocrinol 2020;244:223–36.
[28] Yamada A, Kubo K, Takeshita T, Harashima N, Kawano K, Mine T, et al. Molecular cloning of a glycosylphosphatidylinositol-anchored molecule CDw108. J Immunol 1999;162:4094–100.
[29] Wang L, Song Y, Yi X, Wu C, Guo Q, Zhou X, et al. Semaphorin 7A accelerates the inflammatory osteolysis of periapical lesions. J Endod; 2022.
[30] Korner A, Bernard A, Fitzgerald JC, Alarcon-Barrera JC, Kostidis S, Kaussen T, et al. Sema7A is crucial for resolution of severe inflammation. Proc Natl Acad Sci U S A 2021;118.
[31] Younossi ZM. Non-alcoholic fatty liver disease - a global public health perspective. J Hepatol 2019;70:531–44.
[32] Donnelly KL, Smith CI, Schwarzenberg SJ, Jessurun J, Boldt MD, Parks EJ. Sources of fatty acids stored in liver and secreted via lipoproteins in patients with nonalcoholic fatty liver disease. J Clin Invest 2005;115:1343–51.
[33] Boden G. Obesity, insulin resistance and free fatty acids. Curr Opin Endocrinol Diabetes Obes 2011;18:139–43.
[34] Larder R, Sim MFM, Gulati P, Antrobus R, Tung YCL, Rimmington D, et al. Obesity-associated gene TMEM18 has a role in the central control of appetite and body weight regulation. Proc Natl Acad Sci U S A 2017;114:9421–6.
[35] Zeng N, Bao J, Shu T, Shi C, Zhai G, Jin X, et al. Sexual dimorphic effects of igf1 deficiency on metabolism in zebrafish. Front Endocrinol 2022;13:879962.
[36] Casimiro I, Stull ND, Tersey SA, Mirmira RG. Phenotypic sexual dimorphism in response to dietary fat manipulation in C57BL/6J mice. J Diabet Complicat 2021;35:107795.
[37] Nikkanen J, Leong YA, Krause WC, Dermadi D, Maschek JA, Van Ry T, et al. An evolutionary trade-off between host immunity and metabolism drives fatty liver in male mice. Science 2022;378:290–5.

